Indian Journal of
Applied Radiology

Open Science Publications

Volume 3, Issue 1 - 2017
© Shah DS 2017
www.opensciencepublications.com

Intracranial Nerves Assessment Using 3D Mri Sequences - A Radiologist's Endoscopy - A Pictorial Essay of Intracranial Nerve Anatomy & Pathology

Pictorial Essay

Diva Siddhartha Shah*

Department of Radiodiagnosis, Consultant Radiologist, HCG Cancer Centre, Ahmedabad, India

***Corresponding author:** Dr. Diva Siddhartha Shah, Department of Radiodiagnosis, Consultant Radiologist, HCG Cancer Centre, Ahmedabad, India; Tel: 9428233389; E-mail: drdiva1923@yahoo.co.in

Copyright: © 2017 Shah DS. This is an open access article distributed under the Creative Commons Attribution License, which permits unrestricted use, distribution, and reproduction in any medium, provided the original work is properly cited.

Article Information: **Submission:** 24/07/2017; **Accepted:** 27/08/2017; **Published:** 11/09/2017

Abstract

Intracranial nerve anatomy is complex and requires a detailed understanding of its normal anatomic course for tailoring examinations, locating the abnormalities along its course and interpreting the imaging findings. The aim of this pictorial assay is to emphasize the need of clear knowledge of radiological anatomy of the intracranial nerves for evaluation of cranial neuropathies as well as utility of 3D steady state free precision sequences in evaluation of isolated cranial nerve pathologies. High-resolution isotropic three-dimensional (3D) magnetic resonance imaging acquisition relying heavily on constructive interference in the steady state (CISS) has largely replaced 2D techniques previously used for the evaluation of the intracranial nerves (CNs).

Keywords: CISS; 3D MRI sequences; Intracranial nerves; VIBE; SSFP

Abbreviations

3D: Three Dimensional; ACE: Angiotensin Converting Enzyme; AKT: Anti Koch's Treatment; CECT: Contrast Enhanced Computed Tomography; CISS: Constructive Interference Steady State; CNs: Cranial Nerves; CP angle: Cerebello-Pontine angle; FS: Fat Suppressed; IAC: Internal Auditory Canal; MRI: Magnetic Resonance Imaging; NF-II: Neurofibromatosis II; PCA: Posterior Cerebral Artery; SCA: Superior Cerebellar Artery; SCC: Squamous Cell Carcinoma; SSFP: Steady State Free Precession; VIBE: Volumetric Interpolated Breath-Hold Examination

Introduction

The anatomic visualization of various intracranial nerves largely depends on the nerve diameter, course of the individual nerve as well as on the amount of CSF surrounding it. High-resolution Steady-State Free Precession (SSFP) sequences with a heavily T2-weighted appearance are mainstay of visualization of the cisternal component of the CNs since their introduction by Casselman and colleagues [1]. Casselman et al., first introduced the three-dimensional constructive interference of steady state (3D CISS) sequence for imaging the inner ear and the cerebello-pontine angle [1,2].

Conventional Magnetic Resonance (MR) imaging sequences provide excellent soft-tissue resolution but may lack the spatial resolution which is required for clear depiction of tiny intracranial structures [3,4]. 3D sequences provide submillimetric spatial resolution and high contrast resolution between cerebrospinal fluid and solid structures thus allowing the reconstruction of elegant multiplanar images that highlights the entire course of an individual nerve [4].

The root entry zone, cisternal and intracanalicular segment of each individual nerve is best delineated by non-contrast SSFP sequences [3,4-6,7]. While the interdural and foraminal segments of the CNs are revealed better after the administration of intravenous contrast [3]. Contrast-enhanced T1-weighted images (VIBE-Volumetric Interpolated Breath-Hold Examination) specially help to see the nerves and its branches or segment which are surrounded by venous plexus (III to VI in the cavernous sinus, VI behind the clivus in the basilar plexus, IX to XI in the jugular foramen, XII in the hypoglossal canal) [3,8,9]. On these sequences the intracranial nerve are seen as black structures surrounded by high signal intensity gadolinium-filled venous structures.

Overview of Anatomy

There are 12 paired intracranial nerves, the intracranial segment of paired 12 cranial nerves consists of nuclear, parenchymal fascicular, cisternal, dural cave and interdural segments [5,6]. The identification rate of each cranial nerve is related to difference in its anatomic characteristics, most importantly nerve diameter and intracranial course.

Depending on the diameter cranial nerves can be divided into three groups, first group consist CN's I & II, the second group consist of the CN's III, V, VII, VIII and the lower nerve complex (IX & XI) and the third group consist of the CN's IV, VI, and XII (Tables 1-3) [2,7].

Table 1: Largest diameter nerve group (Intracranial nerve group 1).

Group	Nerves	Important imaging plane and Landmark	Sizes (diameter in mm)
First	Olfactory	It is situated inferior and medial to gyrus rectus and is easily seen in coronal plane (Figure 1)	10 x 4.5 x 2.2 mm
	Optic	It has four anatomic segments. Canalicular segment is the portion that lies in the optic canal, below the ophthalmic artery and should be specifically sought when imaging is done for vision loss (Figures 2A,2B)	5 mm

Imaging Technique

MRI was done on a 1.5-T Siemens Magnetom Symphony Vision in patients with strong clinical suspicion of intracranial nerve involvement. Head coil was used 5 mm thick FSE PD-T2W, FLAIR and T1W axial images, 4 mm FSE coronal T2W & 0.4-0.5 mm thick 3D CISS axial sequences were taken. CISS was taken in every patient for evaluation of cranial nerve segments. Post contrast 4 mm thick SE T1W FS coronal & sagittal as well as 0.4-0.5 mm thick axial FS VIBE sequence (volumetric interpolated breath-hold examination - gradient-echo MR sequence) were acquired for a very smaller enhancing lesion along the course of intracranial nerve.

Discussion

Cranial nerve abnormalities are due to variety of underlying causes (Table 4) [8]. This pictorial essay illustrates the various intracranial nerve involvements by different etiology.

Illustrations

Congenital: A 28 year old male with hearing loss since birth. Axial and coronal T2W images showed a narrow right sided IAC while T2W CISS sequence demonstrated complete aplasia of right vestibulocochlear nerve complex. CISS is considerably superior to 3D Turbo Spin-Echo (TSE) for nerve visualization in the cerebello-pontine angle. The inclusion of CISS in an MRI imaging protocol of the facial and vestibulocochlear nerves is recommended (Figure 11) [10,11].

Infective

Tuberculosis: A 38 year old male with gradual onset of left sided diplopia and blurring of vision along with pulmonary tuberculosis. Abnormal marrow changes and abnormal enhancement seen in left petro-clival region, which may explain the indirect involvement of intracranial nerve. Post contrast VIBE sequence shows abnormal enhancement in of the cisternal segment of left sixth nerve. Patient was given AKT and steroid for intracranial nerve involvement and symptoms were resolved in two months (Figure 12).

Table 2: Intermediate diameter nerve group (Intracranial nerve group 2).

Group	Nerves	Important imaging plane and Landmark	Sizes (diameter in mm)
Second	Occulomotor	It emerges into the interpeduncular cistern & best visualized on oblique axial SSFP images. As it travels between SCA and PCA it is best visualized in coronal plane (Figures 3A,3B).	2.5-3 mm
	Trigeminal	It has a larger cisternal component and SSFP sequence helps in delineating sensory and motor nerve roots. Oblique reformations in individual planes help in delineating its divisions in Meckel's cave (Figures 4A,4B).	2.3-5.4 mm
	Facial	It Runs parallel and superior to the 8th nerve complex, and enters into the internal auditory canal. Its diameter is always lesser than inferiorly lying cochlear nerve on SSFP sagittal oblique images (Figures 5A,5B).	1.8 mm, (range1-2 mm)
	Vestibulo- Cochlear complex	It runs parallel and inferior to the 7th nerve and enters into the internal auditory canal, where it splits into three parts (cochlear, superior vestibular, and inferior vestibular). These three divisions along with the facial nerve have a characteristic appearance on sagittal oblique SSFP cross-sectional images, frequently used for the detection of nerve aplasia/hypoplasia (Figures 5A,5B).	3 mm, (range 2-5 mm)
	Glossopharyngeal & Vagus	They emerge from lateral medulla and run parallel to each other in lateral cerbello-medullary cistern. The cerebellar floculus lies between glossopharyngeal and vestibullo-cochlear nerve complex. Axial oblique and coronal oblique are best planes to visualize the nerves distinctly (Figures 6A,6B).	-
	Spinal Accessory	It consist of multiple cranial and spinal rootlets, spinal rootlets ascends cranially through foramen magnum & into cisterna magna and join the cranial nerve roots in lateral cerebello-medullary cistern. The conjoined nerve root than exits through jugular foramen (Figure 7).	-

Citation: Shah DS. Intracranial Nerves Assessment Using 3D Mri Sequences - A Radiologist's Endoscopy - A Pictorial Essay of Intracranial Nerve Anatomy & Pathology. Indian J Appl Radiol. 2017;3(1): 115.

Table 3: Smallest diameter nerve group (Intracranial nerve group 3).

Group	Nerves	Important imaging plane and Landmark	Sizes (diameter in mm)
Third	Trochlear	It is the thinnest intracranial nerve & the only nerve with root entry zone from dorsal brainstem (Posterolateral to brainstem) (Figure 8).	0.4 mm (range 0.2-0.6 mm)
	Abducent	It courses ventrally through pons into the prepontine cistern, where it is best seen in oblique axial SSFP images, while the petroclival segment is surrounded by venous plexus which is best seen on post contrast 3D T1W axial images (Figures 9A,9B).	2.2 mm (range 1-2.9 mm)
	Hypoglossal	It arises from ventro-lateral sulcus of medulla and runs into lateral cerbello-medullary cistern and exits via hypoglossal canal which is best seen on axial oblique pre or post contrast 3D SSFP or spoiled GRE 3D T1W sequences (Figures 10A,10B).	1.3-1.6 mm

Table 4: Causes of intracranial nerve abnormalities.

Etiology	Causes
Congenital	Aplasia/hypoplasia of nerve
Infective	Tuberculosis, syphilis, leprosy, mycoplasma, Lyme disease, viral infections, fungal infections, parasitic infections.
Inflammatory	Tolosa hunt syndrome, Idiopathic pachymeningitis, sarcoidosis, demyelination diseases.
Physical/Chemical	Radiation, trauma ,Surgery, toxins, drugs
Vascular	Tortous vascular loop, Aneurysm,
Neoplastic - Primary Perineural spread	Schwannoma, neurofibromatosis Primary neoplasm of lung breast or any other malignancy, lymphoma, leukemia

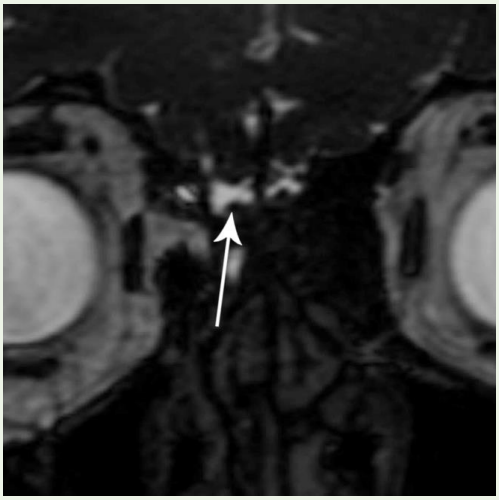

Figure 1: Olfactory nerve- Coronal SSFP 0.5 mm MR images shows olfactory nerve (White arrow) in CSF filled olfactory groove.

Figure 2: Optic nerve -A. Axial oblique 0.5 mm SSFP MR Image shows two out of four segments of optic nerve: The retinal (black arrow), orbital (black arrowheads); B. Canalicular segment of optic nerve (white arrowheads).

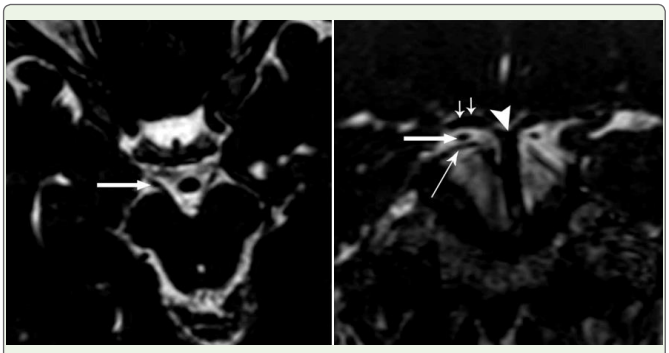

Figure 3: Occulomotor nerve - A. Axial oblique 0.5mm SSFP MR Image shows origin of Occulomotor nerve (white thick arrow) into interpeduncular cistern; B. Coronal 0.5 mm thick MR image shows Occulomotor nerve (white thick arrow) between the posterior cerebral artery (white thin double arrow) & superior cerebellar artery (white thin arrow), basilar artery (white arrow head).

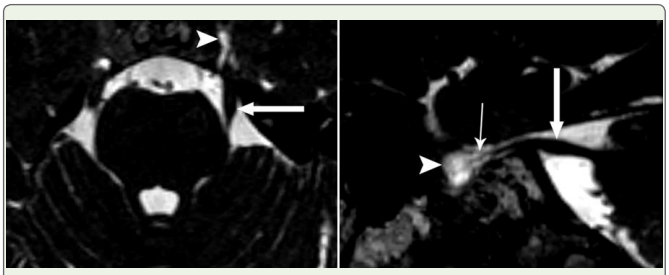

Figure 4: Trigeminal nerve- A. Axial 0.5 mm thick SSFP axial MR image shows cisternal segment (thick white arrow) of trigeminal nerve & it enters into Meckel's cave (white arrowhead); B. 0.5 mm sagittal oblique image shows cisternal (thick white arrow) and divisions of trigeminal nerve (thin white arrow) in Meckel's cave (arrow head).

Citation: Shah DS. Intracranial Nerves Assessment Using 3D Mri Sequences - A Radiologist's Endoscopy - A Pictorial Essay of Intracranial Nerve Anatomy & Pathology. Indian J Appl Radiol. 2017;3(1): 115.

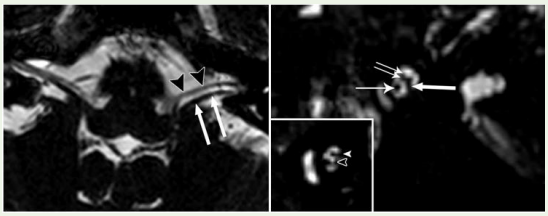

Figure 5: Vestibulocochlear & facial nerve- A. Axial 0.5 mm thick SSFP MR image shows parallel courses of facial (black arrowheads) and vestibulocochlear nerve complex (double thick arrow) in CP angle cistern & enters into internal auditory canal; B. Sagittal oblique 0.5 mm thick SSFP MR image shows common vestibular nerve (thick arrow) facial nerve (thin double white arrow), cochlear nerve (long white arrow) as well as superior & inferior vestibular nerve (white and black arrowheads).

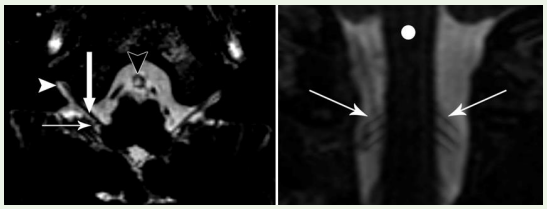

Figure 6: Glossopharyngeal & Vagus nerve- A. Axial 0.5 mm thick SSFP image shows course of right glossopharyngeal (thick white arrow) and vagus nerve (thin white arrow) in lateral cerebello-medullary cistern and enters into the jugular fossa (white arrowhead), Basilar artery (black arrowhead) in prepontine cistern; B. 0.5 mm thick coronal oblique SSFP MR image through cereblo-pontine angle shows glossopharyngeal (thick white arrow) & vagus nerve root (thin white arrow) beneath the flocculus of cerebellum (f).

Figure 7: Spinal accessory nerve- Coronal 0.5 mm thick SSFP image shows spinal rootlets of accessory nerve (white arrow) arising from spinal cord (white circle).

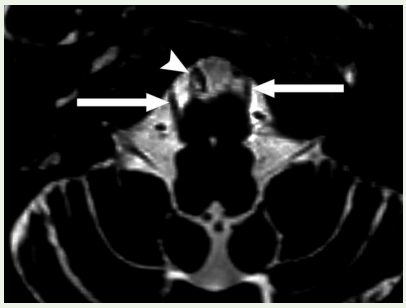

Figure 8: Trochlear nerve- Axial 0.5 mm thick SSFP MR Image shows both trochlear nerve (thick arrow), emerge from dorsal brainstem to cross ambient cistern (white arrow head).

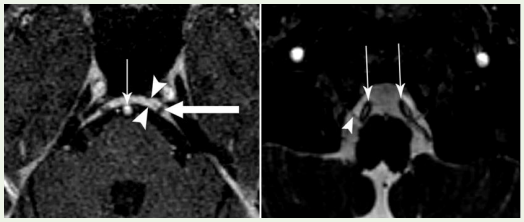

Figure 9: Abducent nerve - A. Oblique axial 0.5 mm thick SSFP MR Image shows both abducent nerve (thick arrow) at ponto-medullary junction; B. Axial post contrast 0.5 mm VIBE image shows petro-clival segment of abducent nerve (thick arrow) in Dollero's canal (arrowhead) white rounded structure represents basilar artery (thin arrow).

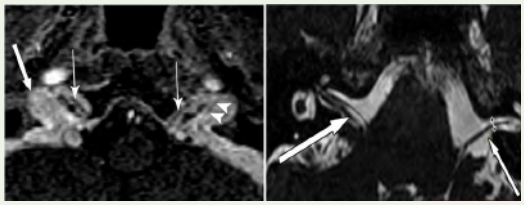

Figure 10: Hypoglossal nerve- A. Axial 0.5mm thick SSFP image shows oblique course of hypoglossal nerve (white arrowhead) in lateral cerebello-medullary cistern and vertebral arteries (thin white arrow) anterior to the nerve; B. Axial post contrast 0.5 mm thick VIBE image shows bilateral hypoglossal nerve (thin arrow) surrounding by venous structures in jugular fossa (thick arrow) & faint glossopharyngeal vagus nerve (white arrowheads).

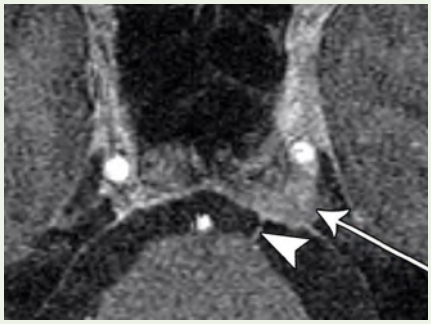

Figure 11: (A 28 year old male with hearing loss) Axial 0.5mm thick SSFP image shows narrowing of right internal auditory canal & non-visualisation of entire course of right vestibulocochlear nerve.

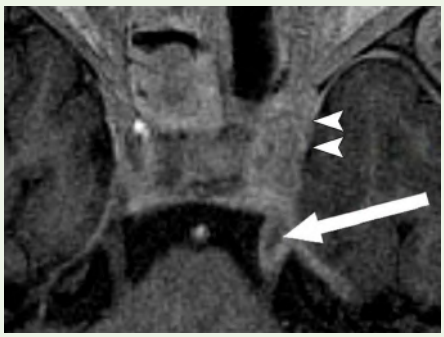

Figure 12: (A 38 year old male with left sided diplopia and blurring of vision) 0.5 mm thick post contrast VIBE axial image shows abnormal enhancement of cisternal part of left abducent nerve (arrowhead) & bulky abnormally enhancing left sided pertro-clival region.

Citation: Shah DS. Intracranial Nerves Assessment Using 3D Mri Sequences - A Radiologist's Endoscopy - A Pictorial Essay of Intracranial Nerve Anatomy & Pathology. Indian J Appl Radiol. 2017;3(1): 115.

Aspergillosis: A 13 year old girl presented with juvenile diabetes having extensive fungal sinusitis with multiple cranial nerve involvement and heterogeneous enhancement involving paranasal sinuses & left cavernous sinus. Post contrast VIBE demonstrated involvement of cisternal portion of left trigeminal nerve as well as left optic nerve involvement & this diagnostic information was helpful as exenteration of globe was considered in view of optic nerve involvement by the fungal infection (Figures 13A,13B).

Inflammatory

Sarcoidosis: A 40 year female with acute onset right sided sixth nerve palsy & headache. MRI brain showed an abnormal pachymeningeal enhancement along the lesser wing of right sphenoid bone and along right cavernous sinus.

Post contrast 3D VIBE sequence revealed an asymmetric & more pronounced enhancement in the posterolateral aspect of right cavernous sinus and in interdural prepontine segment of right sixth nerve (Dorello's canal), which very well explained acute onset of sixth nerve palsy. Patient's serum ACE levels were high diagnosed as neurosarcoidosis and responded well with steroids (Figures 14A,14B).

Tolosa-hunt syndrome: A 55 year old male with left sided multiple cranial nerve palsy (3rd, 4th & 6th). MRI brain revealed asymmetric bulky and abnormal enhancement involving left orbital apex, superior orbital fissure and cavernous sinus which is well demonstrated by pre-contrast SSPF sequence and post contrast VIBE images. The imaging findings of Tolosa-Hunt syndrome are classical but may be subtle. Conventional MRI may show only slight enlargement or alteration in the shape of the cavernous sinus but this is well seen on a CISS sequence (Figures 15A,15B) [11].

Physical/Chemical

Post radiation: A 45 year old female with known right sided trigeminal neuralgia since six years underwent radiosurgery for ablation of right sided trigeminal nerve. Post procedure MRI was done showed focal enhancement and fuzzy margins of right trigeminal nerve in its cisternal portion just proximal to its entry in to the Meckel's cave (Figure 16). The enhancement represents radiation dose effect at targeted site. The trigeminal nerve enhances at the target site after radiosurgery. 3D post contrast T1W MR Imaging is useful to confirm the presence and location of the treatment site after radiosurgery for trigeminal neuralgia [12-14].

Vascular: A 62 year old female with pain and paraesthesia over left side of face. Heavily T2W steady state free precision sequence showed an atrophied left sided sensory and motor nerve root of trigeminal nerve with a vascular loop of left superior cerebellar artery indenting cisternal portion of left trigeminal nerve. Right trigeminal nerve was normal.

Trigeminal neuralgia is caused most commonly by compression of the root entry zone of the trigeminal nerve by a vascular loop [12]. This compression and displacement of the nerve by the vascular loop is well evaluated by the CISS sequence (Figures 17A,17B) [11].

Neoplastic

Primary: A 72 year old male with left sided sensorineural hearing loss and positional vertigo diagnosed with a large heterogeneously

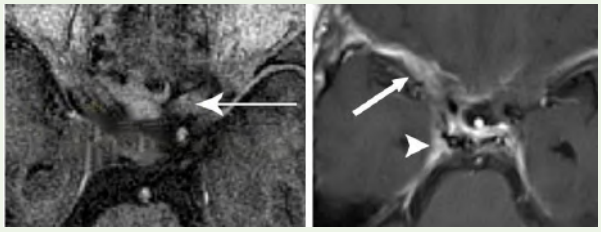

Figure 13: (13 year old girl with juvenile diabetes and fungal sinusitis) A. 0.5 mm thick post contrast axial VIBE image shows bulky & abnormal enhancement of cisternal portion of left trigeminal nerve (thick white arrow), left cavernous sinus (white arrowheads); B. 0.5mm thick post contrast T1W image shows abnormal heterogeneous enhancement of canalicular portion of left optic nerve (thin white arrow).

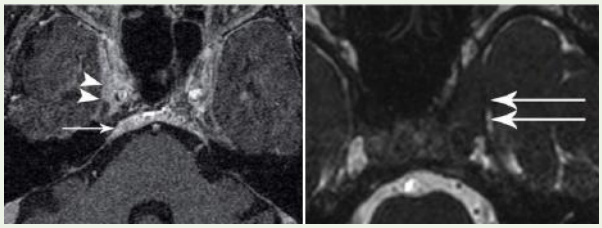

Figure 14: (40year old female with acute onset of right sixth nerve palsy) A. 3mm thick axial post contrast T1W MR Image shows abnormal pachymeningeal enhancement along the lesser wing (thick white arrow) and cavernous sinus (arrow head) on right side; B. 0.5 mm thick post contrast T1W VIBE image shows abnormal and asymmetric enhancement in posterolateral aspect of cavernous sinus (white arrowhead) and interdural segment (Dorello's canal) of right sixth nerve (thin white arrow).

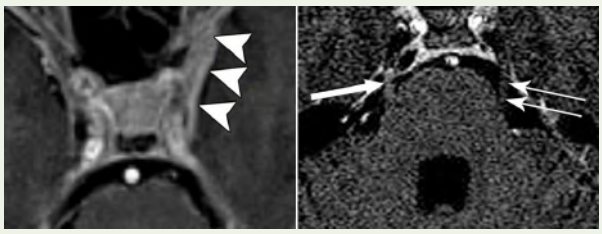

Figure 15: (A 55 year old male with left sided 3rd,4th & 6th nerve palsy) A. pre-contrast 0.5mm thick axial SSFP image shows bulky and isointense signal in left cavernous sinus (thin white arrows); B. Post contrast 0.5 mm thick T1W image shows abnormally enhancing signal in left cavernous sinus & left superior orbital fissure (white arrowhead).

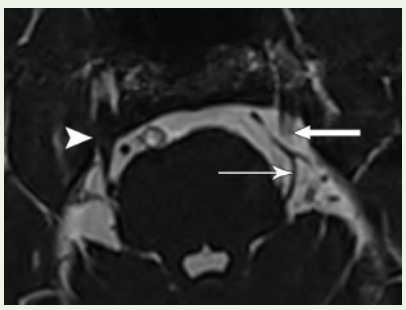

Figure 16: (45 year old female known case of right trigeminal neuralgia, post ablation) Post contrast 0.5 mm thick axial T1W FS VIBE image shows abnormally enhancing and fuzzy margin of cisternal segment of right trigeminal nerve (thick white arrow) , normal cisternal portion of left trigeminal nerve (thin white arrows).

Citation: Shah DS. Intracranial Nerves Assessment Using 3D Mri Sequences - A Radiologist's Endoscopy - A Pictorial Essay of Intracranial Nerve Anatomy & Pathology. Indian J Appl Radiol. 2017;3(1): 115.

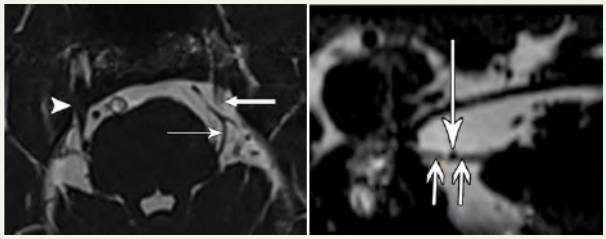

Figure 17: (A 62 year old female with pain and paraesthesia over left side of face) A. 0.5 mm thick axial SSFP image shows markedly atrophied root entry zone & cisternal portion of left trigeminal nerve (thick white arrow) and a vascular loop of left superior cerebellar artery crossing the cisternal portion of left trigeminal nerve (thin white arrow). White arrowhead represents normal right sided trigeminal nerve; B. Sagittal oblique 0.5mm thick SSFP image shows atrophied left trigeminal nerve (thin small white arrows) and flow void of SCA superior to it (thin white arrow).

enhancing vestibulocochlear schwannoma in left CP angle cistern having extension into the left internal auditory canal. It is well depicted on high resolution 3D CISS and on post contrast VIBE sequences. Acquiring images in the coronal and oblique sagittal planes perpendicular to the IAC proved to be most useful for demonstrating the location of the lesion (Figure 18).

A 28 year old patient with NF-II showing larger right sided vestibulocochlear nerve schwannoma and on left side only intracanalicular schwannoma of vestibular nerve origin. It is well depicted on oblique multiplanar reformations of CISS sequence and shows enhancement on post contrast 3D T1W FS sequence (Figures 19A,19B). SSFP sequence gave the maximum information concerning the spatial relationship of the small intracanalicular tumor. Acquiring images in the coronal and oblique sagittal planes perpendicular to the IAC proved to be most fruitful for demonstrating the location of the lesion [13].

Perineural spread: A 67 year old male with neuroendocrine tumor of anterior mediastinum, presented with acute onset of dysphagia and dysphonia and suspected lower cranial nerve palsy. Conventional MRI brain sequences did not show any abnormality. SSFP technique showed a nodular lesion at origin of 9th, 10th cranial nerve complex with homogenous enhancement appreciated in thinner post contrast fat sat T1W images (Figures 20A,20B).

A 70 year old male patient treated for SCC of lung presented with acute right sided 7th nerve palsy and headache. Conventional MRI brain sequences showed basal leptomeningeal enhancement along left sided basal cisterns, which did not explain right sided 7th nerve palsy. A CISS sequence reveals a nodular and thickened abnormally enhancing cisternal segment of right sided facial nerve and it showed nodular enhancement on thin post contrast VIBE T1W fat saturated images (Figures 21A,21B).

A 46 year old female operated for carcinoma of breast with pain in right side of face radiating up to the right ear. T2W FSE images showed subtle abnormality in right sided Meckel's cave, while CISS demonstrates bulging and abnormal signal in right sided of Meckel's cave with non-visualization of divisions of trigeminal nerve and it showed abnormal heterogeneous enhancement on post contrast scan. Cisternal portion of right trigeminal nerve was uninvolved (Figures 22A,22B).

Figure 18: (72 year old male with left sided sensorineural hearing loss & vertigo) Axial 0.5mm thick SSFP image shows complex solid cystic lesion in left CP angle cistern (thick arrow) and extension into left internal auditory canal (thin arrow).

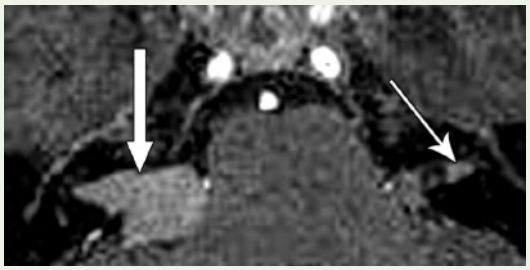

Figure 19: (28 year old patient with neurofibromatosis-II) Axial 0.5mm SSFP image shows isointense schwannoma in right CP angle cistern and extending into right internal auditory canal (thick white arrow) & small lesion in left internal auditory canal (thin white arrow).

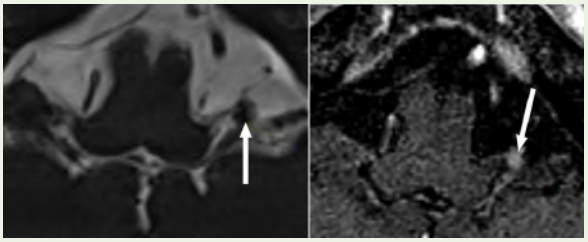

Figure 20: (67 year old male patient with neuroendocrine tumor of anterior mediastinum with acute onset of dysphagia and dysphonia) A. 0.5mm thick axial SSFP image shows isointense nodule at origin of left 9th and 10th nerve root entry zone (thick white arrow); B. 0.5mm thick post contrast VIBE image shows enhancing nodule at left root entry zone of 9th & 10th cranial nerves (thick white arrow).

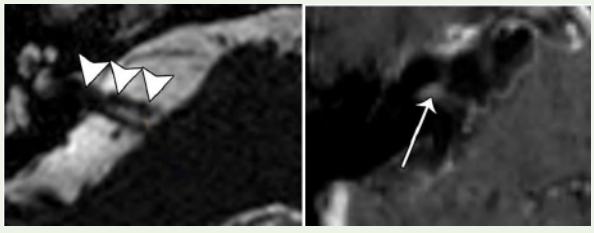

Figure 21: (70 year old male known squamous cell carcinoma of lung presented with acute right sided 7th nerve palsy) A. 0.5mm thick axial SSFP image shows nodular & thickened cisternal segment of right facial nerve (white arrowheads); B. 0.5 mm thick post contrast VIBE image shows nodular enhancement of right facial nerve (thin white arrow).

Citation: Shah DS. Intracranial Nerves Assessment Using 3D Mri Sequences - A Radiologist's Endoscopy - A Pictorial Essay of Intracranial Nerve Anatomy & Pathology. Indian J Appl Radiol. 2017;3(1): 115.

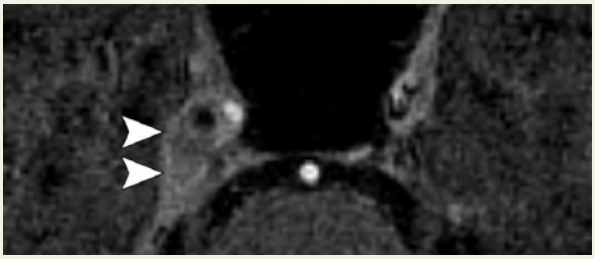

Figure 22: (46 year old female treated for carcinoma of breast presented with severe pain on right side of face) 0.5mm thick axial SSFP image shows bulky and isointense signal in right Meckel's cave (thick white arrow), normal divisions of left trigeminal nerve in left Meckel's cave (thin arrow).

Conclusion

Imaging of the CNs presents a challenge due to their small size and course. Cisternal and canalicular segments are best visualized by precontrast SSFP sequences, while interdural segment is best seen with post contrast spoiled gradient echo T1W FS sequences or post contrast enhanced SSFP sequences. High resolution 3D MR sequences act as radiologist's endoscope for evaluation of pathologic processes involving various segments of the intracranial nerves.

References

1. Casselman JW, Kuhweide R, Deimling M, Ampe W, Dehaene I, et al. (1993) Constructive interference in steady state-3DFT MR imaging of the inner ear and cerebellopontine angle. Am J Neuroradiol 14: 47-57.
2. Yousry I, Camelio S, Schmid UD, Horsfield MA, Wiesmann M, et al. (2000) Visualization of cranial nerves I-XII: Value of 3D CISS and T2-weighted FSE sequences. Eur Radiol 10: 1061-1067.
3. Casselman J, Mermuys K, Delanote J, Ghekiere J, Coenegrachts K (2008) MRI of the cranial nerve more than meets the eye: Technical considerations and advanced anatomy. Neuroimaging Clin N Am 18: 197-231.
4. Sheth S, Branstetter BF, Escott EJ (2009) Appearance of normal cranial nerves on steady-state free precession MR images. Radiographics 29: 1045-1055.
5. Blitz AM, Macedo LL, Chonka ZD, Ilica AT, Choudhri AF, et al. (2014) High-resolution CISS MR imaging with and without contrast for evaluation of the upper cranial nerves: Segmental anatomy and selected pathologic conditions of the cisternal through extraforaminal segments. Neuroimaging Clin N Am 24: 17-34.
6. Soldatos T, Batra K, Blitz AM, Chhabra A (2014) Lower cranial nerves. Neuroimaging Clin N Am 24: 35-47.
7. Hasan Aydin, Alper Dilli, Elif Altin, Serdar Sipahioğlu, Baki Hekimoğlu (2010) Visualization of cranial nerves, V-VIIIth with MRI; value of b-FFE, T2W drive, T2W TSE and post contrast T1W sequences. Turkiye Klinikleri J Med Sci 30: 1827-1836.
8. Saremi F, Helmy M, Farzin S, Zee CS, Go JL (2005) MRI of cranial nerve enhancement. Am J Roentqenol 185: 1487-1497.
9. Block KT, Chandarana H, Fatterpekar G, Hagiwara M, Milla S, et al. (2013) Improving the robustness of clinical T1-weighted MRI using radial vibe magnetom flash.
10. Yousry I1, Moriggl B, Schmid UD, Naidich TP, Yousry TA (2005) Trigeminal ganglion and its divisions: Detailed anatomic MR imaging with contrast-enhanced 3D constructive interference in the steady state sequences. Am J Neuroradiol 26: 1128-1135.
11. Hingwala D, Chatterjee S, Kesavadas C, Thomas B, Kapilamoorthy TR (2011) Applications of 3D CISS sequence for problem solving in neuroimaging. Indian J Radiol Imaging pp. 90-97.
12. Becker M, Kohler R, Vargas MI, Viallon M, Delavelle J (2008) Pathology of the trigeminal nerve. Neuroimaging Clin N Am 18: 283-307.
13. Thomas B, Krishnamoorthy T, Arvinda HR, Kesavadas C (2008) 3D-CISS MRI in a purely intracanalicular cochlear schwannoma. J Neuroradiol 35: 305-307.
14. Alberico RA, Fenstermaker RA, Lobel J (2001) Focal enhancement of cranial nerve V after radiosurgery with the leksell gamma knife: Experience in 15 patients with medically refractory trigeminal neuralgia. AJNR Am J Neuroradiol 22: 1944-1948.

Citation: Shah DS. Intracranial Nerves Assessment Using 3D Mri Sequences - A Radiologist's Endoscopy - A Pictorial Essay of Intracranial Nerve Anatomy & Pathology. Indian J Appl Radiol. 2017;3(1): 115.